DETECTION OF IN-FLIGHT ICING CONDITIONS THROUGH THE
ANALYSIS OF HYDROMETEORS WITH A VERTICALLY POINTING RADAR

Jennifer Lilly, Frédéric Fabry
McGill University, Montreal, Quebec, Canada

1. CHALLENGE

In the 100 years since the Wright Brothers first flew a powered aircraft, aviation has not only exploded in popularity, but also has faced many challenges. Since 1931 when icing was first suggested as a possible accident explanation, aircraft icing has been recognized as a significant aviation hazard. Despite extensive research and regulations by the US government, in the last several years (1982 to 2000) there were almost 700 lives and over 450 planes lost in US general aviation accidents where icing played some role (Petty et al., 2003). In the United States alone, an average of 24 accidents, 30 fatalities and 96 million dollars in damage result from icing related accidents each year (Paull and Hagy, 1999). Because of these disturbing statistics, pilots, engineers, air traffic controllers and meteorologists continue to work towards the prevention of aircraft icing.

2. APPROACH

Icing systems generally take one of two forms, a large scale approach based on the interpretation of model, satellite, and / or scanning radar data, or a small scale approach based on specific technology and dedicated hardware. Considering the fact that 95% of all icing accidents take place in the approach, landing, holding, or go around phase of flight (Hallett, 2002) this study uses a vertically pointing radar (VPR) to provide icing information in the vicinity of the airport, where problems most often occur.

In order to successfully identify icing conditions there are five main combinations of hydrometeors that must be recognized: 1) liquid cloud with no drizzle and no ice, 2) liquid cloud with drizzle and no ice, 3) liquid cloud hidden in snow or ice cloud, 4) liquid cloud and drizzle hidden in snow or ice cloud, 5) freezing drizzle or rain. Detecting and identifying the type of precipitation, separating out any mixed precipitation, and quantifying the amount of supercooled liquid water (SLW) are the main challenges put to any icing system. Radar is the only tool with good ranging abilities that can distinguish hydrometeors; however, since icing often occurs hidden within other types of precipitation, radar data alone are not enough to

Corresponding author address: Frédéric Fabry, Dept. of Atmospheric and Oceanic Sciences, McGill University, Montreal, QC, H3A 2K6 Canada;
frederic.fabry@mcgill.ca

identify icing. Systems that are only based on scattering or propagation based approaches, or that try to address a very large area are often unable to separate these five groups of precipitation, and thus encounter problems when identifying icing. Using fall velocities, reflectivities, and spectra data from the VPR, combined with a temperature profile the system presented in this paper has a unique ability to recognize each of these situations. Thus, despite the fact that it is nearly impossible to observe SLW under all conditions with active remote sensors; there are enough clues from the VPR that a series of algorithms can be developed to detect not only the location of SLW, which leads to icing, but also the severity of the icing, or the amount of SLW.

This study aims to minimize icing dangers by creating a robust, real time, accurate, automated system which uses VPR data and meteorological theory to reduce or even prevent aviation accidents related to icing. First all mixed precipitation is separated, then a set of classification algorithms is applied to the data, to detect and distinguish different types of hydrometeors finally the SLW content can be calculated in any areas of frozen precipitation with the Snow Flux Gradient (SFG) or the Snow Density Gradient (SDG) algorithms.

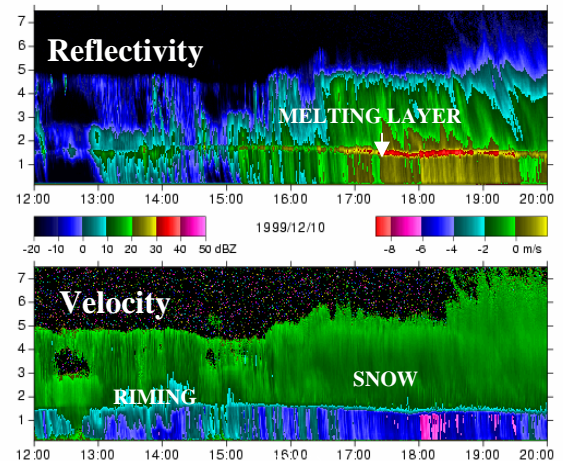## 3. IDENTIFYING AND SEPARATING TARGETS

Figure 1. *Time-height section of radar reflectivity (top) and vertical velocity (bottom) in precipitation. In this example, one can observe a variety of types of precipitation including snow, rain, and rime. Furthermore, the presence of some of these observed hydrometeors such as rimed snow imply the presence of invisible liquid clouds. At 2 km, between 1700 and 1930, a bright band indicates snow clearly melting into rain.*

The above image shows reflectivity (Z), Doppler velocity (v) from the VPR on December 10th 1999. While reflectivity and velocity data allow regions of snow, rain, drizzle, riming, and melting to be identified, it does not offer enough information about regions of mixed precipitation. To gather information about these regions, which are the most likely to have icing, it is necessary to look at the spectra data also available from the VPR (Fig. 2).
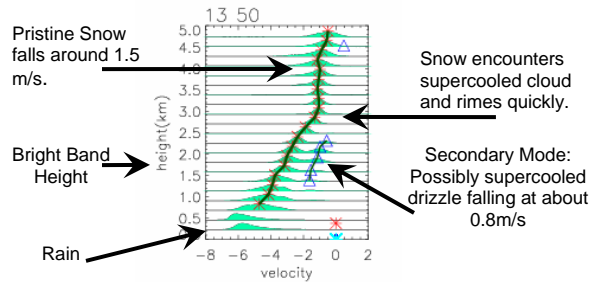

Figure 2. *This is a vertical profile of the vertical velocity spectrum for a ten-minute period starting at 1350 on December, 10th 1999. Each of the 20 curves illustrates, at different altitudes, the relative contribution of targets with a given vertical velocity. At 5 km snow is falling with a typical fall velocity of 1.5m/s (negative is towards the ground), however below 3km the snow encounters SLW and rimes. At this point the snow's fall velocity steadily increases as the ice crystals collect large amounts of cloud droplets becoming increasingly denser. In parallel, a secondary mode shown in blue is observed and is probably caused by supercooled drizzle, a greater hazard to aviation than supercooled cloud by itself.*

By searching the 128 bin spectra data at each height and time for individual peaks in power returned, modes can be identified. Mixed precipitation can be identified as areas with more than one mode. Looking for vertical patterns in spectra data also helps to segregate mixed precipitation and identify regions of SLW. From this point forward, groups will be refer to as a set of peaks in spectra data that are consistent in height (in other words the peaks do not vary by more than .5m/s over 75m).

Once the modes have been separated the next step is to apply a series of classification algorithms. The bright band (BB) algorithm is applied first to the data in general, and then the snowscore, rimescore, drizzlescore and rainscore algorithms are applied to the data once it has been separated into groups.

In this study finding the BB is the first step in teaching the computer to look at radar data the way a meteorologist looks at a radar image. For a meteorologist, the BB stands out as one of the most obvious features on a radar image, and provides understanding that the area above the BB is dominated by frozen precipitation and the area below

the BB is generally rain. To make an automated system, a computer must be trained to use the available information, in this case reflectivity, fall velocity, and temperature, to identify the BB and then like humans make conclusions based on where the BB is located.

For all the classification algorithms, fuzzy logic allows the computer to interpret the VPR data much like a person. In the case of the BB, fuzzy logic allows us to answer the question: is there a BB, and if so, where is it? Fuzzy logic is a rules based system that determines the degree to which something is true. A problem is broken down to the simplest criteria and then a set of rules is established to judge each criterion, and finally another set of rules is established to combine the values of each individual criterion into a final answer. In this way the computer not only has a gray area between black and white, but also can make conclusions with incomplete, imprecise, vague, ambiguous, or noisy data.

In the case of the BB the fuzzy logic criterion are temperature, derivative of velocity, and the presence of a local maximum in Z (Rscore). Temperature can be derived from sounding data or model data and must be interpolated to have the same time and height as the radar data. This study uses only sounding data, which was available because of the AIRS field project; however, in many other circumstances the result would be better with model data that has better time and space resolution. The derivative of velocity shows the change in velocity with height, thus the peak of the derivative of velocity shows the area where the particles collapse from snowflakes into raindrops and begin to fall quickly. Reflectivity score (Rscore) is calculated in equation (1) by taking a reflectivity value and subtracting the average of the points 150m above and below it.

$$\text{Rscore} = Z_h - \frac{(Z_{h+150} + Z_{h-150})}{2} \qquad (1)$$

Rscore gives a value to the peak in reflectivity. This peak is usually found where the snowflakes first start to melt, because at that point they still maintain their larger snowflake shape, but are covered in a layer of liquid, thus increasing their $\|K^2\|$ value from .21 to .93.

The rules for each factor are fairly simple in this case. Each factor has a cut off point where no BB is possible, and is given a score of zero; plus each factor has a point where conditions are ideal for the formation of a BB, and a score of one or 100%, is given. In all cases there is a simple linear transition between the cut off point and 100% point. The criteria used for each score are shown in Fig. 3. Finally the rules for combining each criterion into an algorithm are explained.
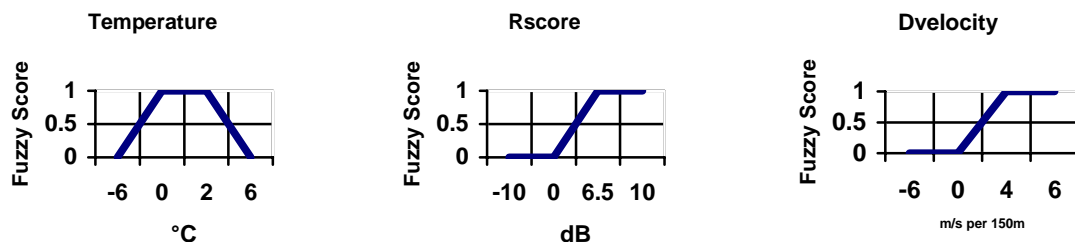
Figure 3: *Fuzzy Logic BB rules. These three graphs show the fuzzy cut of points for the bright band algorithm. Ideal conditions for the BB occur when temperature is between 0-2°C, Rscore is greater then 6.5dB and Dvelocity is greater than 4m/s per 150m.*
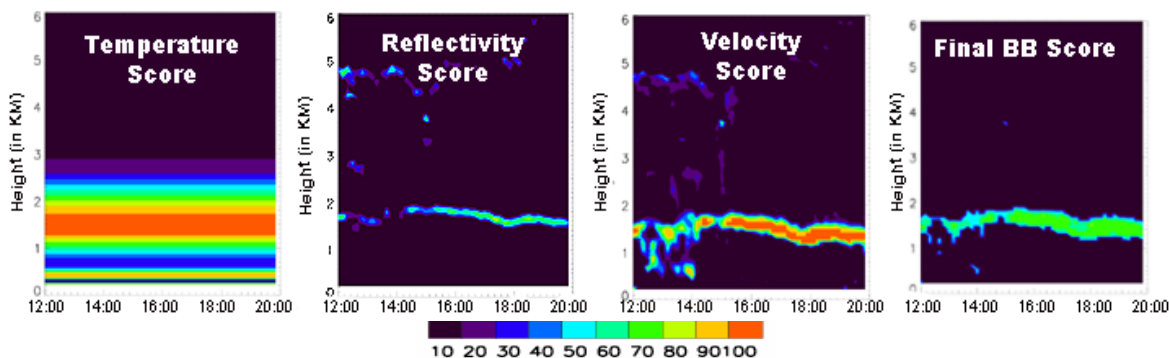

Figure 4: *BB Scores. This figure shows the score for temperature, velocity, and reflectivity (from left to right). Red indicated a score of 1 and black a score of 0. By combining these in a 20%, 50%, 30% ratio, with velocity 300m below reflectivity and temperature, a bright band is calculated by the fuzzy logic algorithm. The greenblue bright band on the right is a combination off all the areas that have a score of 50% or higher when the three factors are combines in the manner described. When compared to figure 1 the algorithm creates a good representation of when was seen in the data.*

The logic behind the limits was based in observation and the physics of what causes a melting layer. The temperature cut off points are -6°C or 6°C, and the 100% points are between 0°C and 2°C. These two bounds were chosen as the levels where melting just begins and the level where melting must be finished. The peak area the BB is usually found just below, or on the warm side of the zero degree isotherm, thus the 100% fuzzy logic score was given in the region of 0°C to 2°C (Stewart et al, 1984). For reflectivity, the cut off point was chosen as a 0 dB peak over 300 meters and the 100% point was chosen as a 6.5 dB peak over 300 meters. The limit of 6.5 dB was chosen in part because melting leads to a change in the $\|K^2\|$ value that would correspond to 6.5 dB, and in part because 6 dB was observed frequently, in case studies of the BB, as the change in reflectivity over the BB (Fabry and Szyrmer, 1999). Finally for the derivative of velocity, the cut off point was chosen as 0, and the 100% point was chosen as a change of more than 4 m/s over 150 m (between any two velocity points). This corresponds to the typical change of fall speed between rain (6m/s) and snow (1.5m/s)

Having established rules and obtained results for each factor (see Fig. 4), the factors must now be combined with another set of rules. In this study the BB rules use 20% temperature, 30% reflectivity, and 50% velocity, with temperature and reflectivity at the same height and

velocity 300 meters below. Temperature is only given a 20% value because the data was collected at a much lower resolution and the range of temperatures where a BB could be found was large. Reflectivity is affected by particle size, particle concentration, shape, orientation, and density effects (Fabry and Zawadzki 1995) and thus can change for many reasons while velocity changes occur mostly because of a change in state. For this reason velocity is weighted the most at 50% while reflectivity and temperature are weighted correspondingly less.

Once the BB is established, the next step is to automatically identify precipitation types as viewed by the radar, and it is done in much the same way the BB is identified. By merging data from the past several years, a picture of precipitation types emerges for each velocity reflectivity combination (see Fig. 5). Some areas of the figure are clearly one type of precipitation, like the high velocity, high reflectivity areas of rain, and the low reflectivity, zero velocity area of cloud. However, there are also areas of average reflectivity and average velocity which are typical of mixed precipitation and can be among other things snow, drizzle, rimed snow, or ice pellets. Thus fuzzy logic algorithms were designed using reflectivity, velocity, and temperature to identify a score in all regions for snow, rain, rime, and drizzle. The results from the BB algorithm also contribute to the classification algorithms

since rain is only possible below a BB, and snow could only occur above the BB or when there was no BB. The specific details of each algorithm, including the given limits, are available in Lilly (2004).
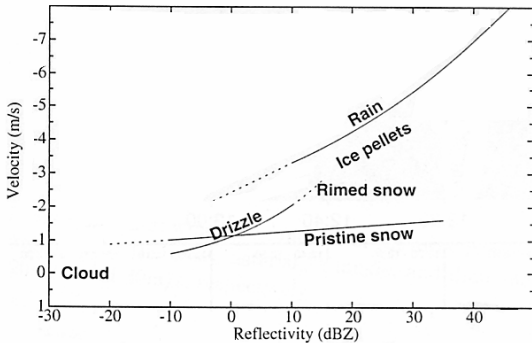

Figure 5. *Radar reflectivity and vertical velocity measurements associated with different types of targets in the absence of vertical air velocity. (Fabry et al, 2003)*

Once all the algorithms have run, a final ID can be given to each area of precipitation. This final ID was simply chosen based on which algorithm has the highest score in a given region. An example of the final ID can be seen in Fig. 6.
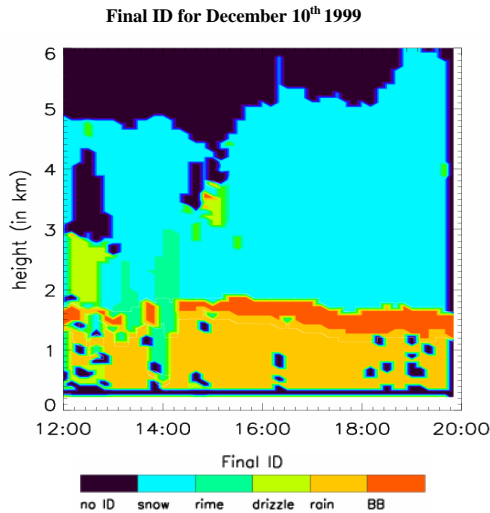
Figure 6. *Final ID for the dominant type of precipitation. IDs are given to all cases of mixed precipitation, but are not shown in this figure.*

4. QUANTIFYING ICING IN SNOW

Having separated out the mixed precipitation and identified the type of precipitation, the last step is to quantify the amount of SLW. While the VPR itself does not provide enough information to explicitly recognize the severity of icing, two algorithms, the snow flux gradient (SFG) and the snow density gradient (SDG),

provide a good estimate of the amount of SLW. These two algorithms infer the amount of SLW by looking at how much riming is occurring. Thus the two algorithms are only valid when SLW is mixed with another type of frozen precipitation.

The SFG algorithm uses mass, derived from reflectivity, to calculate the liquid water content (LWC). Specifically:

$$LWC = \underbrace{\frac{1}{\beta M_s^{0.82}}}_{1^{st}} \underbrace{\frac{\partial Ms \overline{V}s}{\partial h}}_{2^{nd}}, \qquad (2)$$

where the second term is the change in mass flux with height and the first term is a thermodynamic term. The complete derivation is given in Zawadzki et al (2000). If the flux growth exceeds what is expected from deposition and aggregation, riming occurs. The speed at which riming is occurring allows a calculation to provide an estimate of the amount of SLW. Figure 7 gives an example of the results of the SFG algorithm.
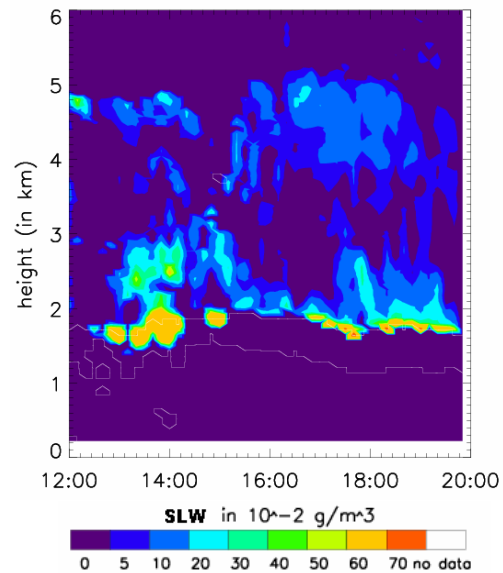

Figure 7. *SFG shows a max in LWC around 1350 which is the same time drizzle was visible in the spectra plots.*

The SDG algorithm uses density to make an estimate of SLW based on the amount of riming. Assuming a snowflake size distribution, the SDG calculates rainfall-equivalent fall speed, then, using the ratio of v(snow) and v(rain equivalent), derives the density of snow. Finally, from the increase in observed snow density, it provides information on the level of riming. In this way the SDG uses fall speed increase, caused by the increase in snowflake density from riming, to calculate the amount of liquid water (LWC). Specifically,

$$LWC = \underbrace{\frac{d\rho}{dh}}_{1^{st}} \underbrace{\frac{4r_s}{3E}}_{2^{nd}}, \qquad (3)$$

where the first term is the change in snowflake density with height and the second term includes r_s the radius of a snowflake and E, the accretion efficiency. A more detailed explanation of this algorithm can be found in Lilly (2004), or Veccei (2002). Figure 8 gives an example of the results of the SDG.
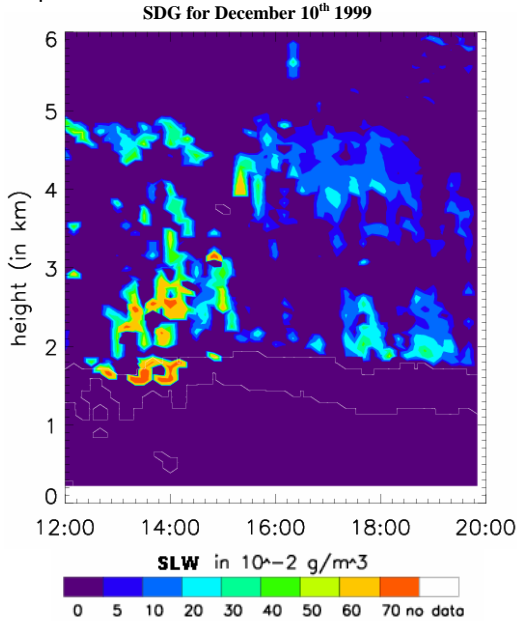
SDG for December 10th 1999

SLW in 10^-2 g/m^3

0   5   10   20   30   40   50   60   70 no data

Figure 8. Like the SFG, SDG shows a max in LWC around 1350 which is the same time drizzle was visible in the spectra plots.

While both algorithms are good, the SFG is more likely to be misled by aggregation.

5. VERIFICATION

While these algorithms have been designed to work in many different types of conditions, it is useful to see how they perform on an interesting day. Thus this paper has attempted to offer a kind of case study for December 10th 1999 by following each explanation with examples from the same date and time period.

The raw data are presented in Fig. 1 and Fig. 2. Note in Fig. 1 the clear areas of snow followed by melting and rain at the end of the period and the more ambiguous regions of rimed snow and possibly drizzle early in the time period. Fig. 2 and Fig. 6 confirm these observations. Looking ahead to Fig. 6 the automatic ID fits well with the observations, while Fig. 2 provides information on the regions of mixed precipitation that are not clear in the raw data. The spectra, shown in Fig. 2, from 1350, have the most interesting 10 minute time

period on this day in terms of icing. The spectra not only calls out attention to the information hidden in the raw ZV plots, but also highlights the need for separating out mixed precipitation.

In order to calculate the values of LWC, the SFG (Fig. 7) and the SDG (Fig. 8) are run on the areas of frozen precipitation as identified in Fig. 6. To validate these results Fig. 9 shows a plot of integrated liquid water content (ILWC) from the SDG (pink), the SFG (red), and two radiometers, (light blue is the WVR-1100, and dark blue is the TP/WVP3000). However since radiometers do not work well in the rain, a comparison with the radiometer for this day does not give very much information.
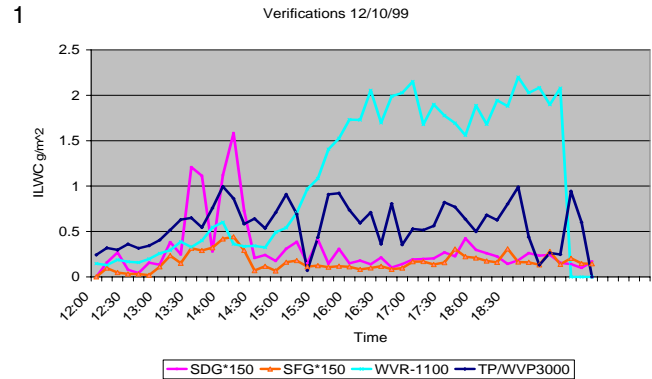
1

Figure 9. Like the SFG, SDG shows a max in LWC around 1350 which is the same time drizzle was visible in the spectra plots.

6. CASE STUDY

December 13th, 1999, from AIRS1, offers a better example to investigate the usefulness of these algorithms. December 13th has no rain to interfere with the results given by the radiometers, and there is at least an hour of supercooled drizzle aloft.
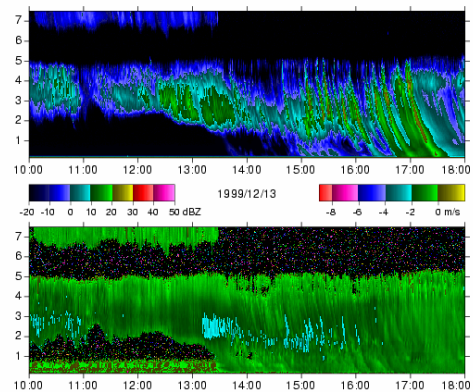

Figure 10. Time-height section of radar reflectivity (top) and vertical velocity (bottom) in precipitation. In this example, there is no bright band, but the fast fall velocities before 1400 draw suspicions of SLW.

From the raw data above (Fig. 10) it is clear that there is no rain; however there is only a hint of the region of SLW hidden between 1300 and 1500, this is not enough information to make any icing judgments. Thus we once again look to the spectra (Fig. 11) before applying the classification algorithms.
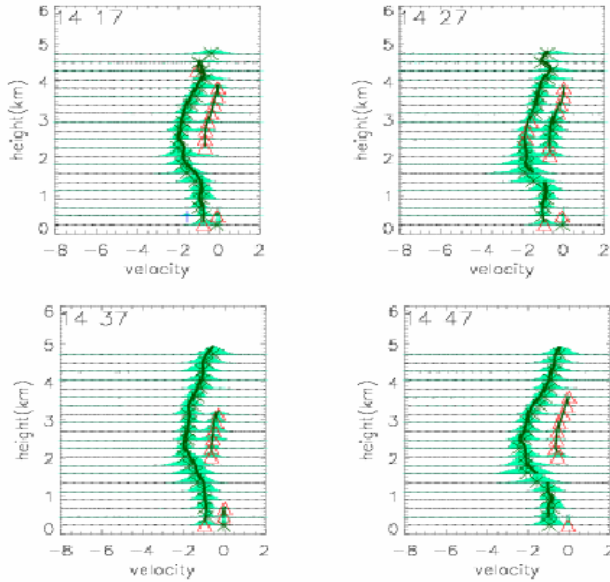

Figure 11. *Spectra with double modes for 12/13/99*

The spectra show a clear secondary mode, and thus for each group the classification algorithms are applied in the same manner as was done for December 10th 1999. Finally to all areas of frozen precipitation the SFG (fig. 12) and SDG (Fig. 13) algorithms are applied.
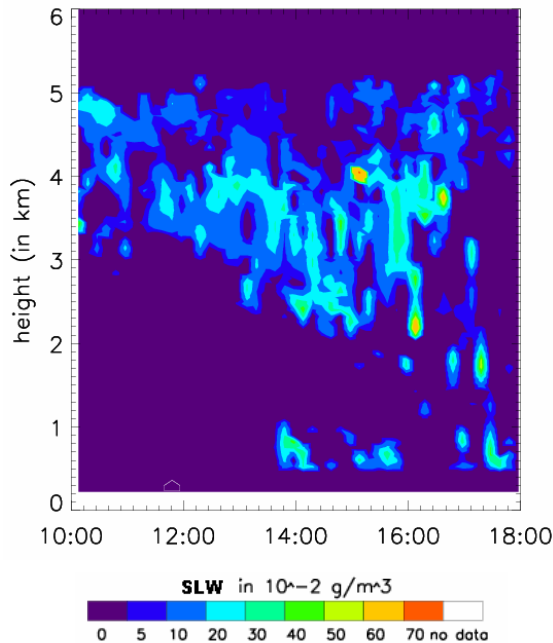

Figure 12. *SFG shows a max in LWC around 1410 which is the same time drizzle was visible in the spectra plots.*
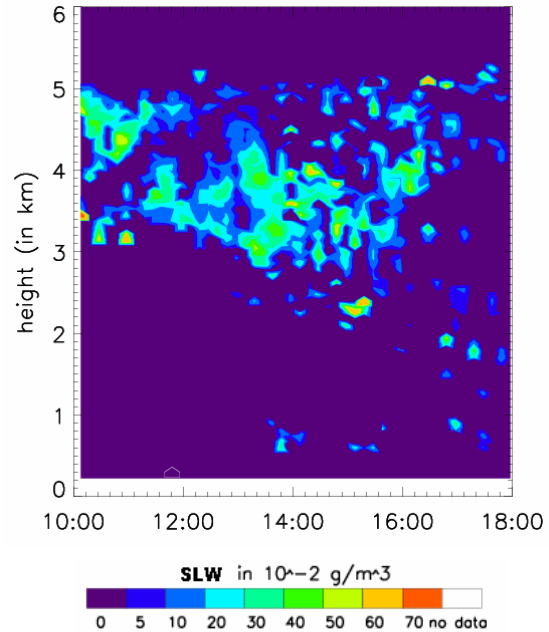

Figure 13. *Like the SFG, SDG shows a max in LWC around 1410 which is the same time drizzle was visible in the spectra plots.*

The results of these algorithms can be verified by plotting them against radiometer data (Fig. 14).
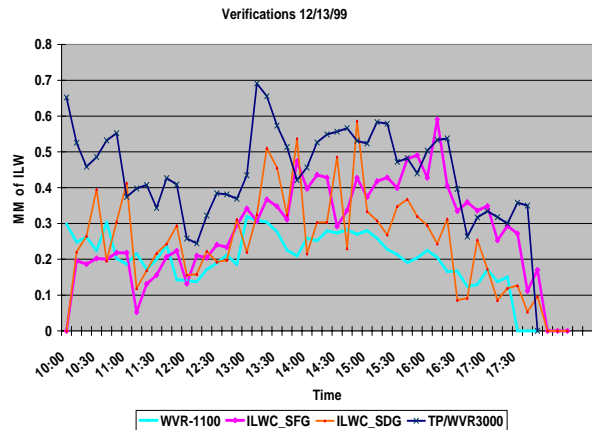

Figure 14: *These verifications show the results of the algorithms falling between the results of the two radiometers.*

7. CONCLUSIONS

The use of these algorithms with a dedicated vertically pointing radar, alone or as part of a complex system, can essentially be used to detect even the most complex icing situations. It is yet to be determined the extent with which the spatial variability of SLW in the atmosphere will affect the representativeness of estimates made by this approach or any other approach that uses measurements obtained from a single pointing direction.

8. REFERENCES

Fabry, F., I. Zawadzki, S. Cober, G. Isaac, T. Ratvasky, F. Solheim, 2003: Detection of In-Flight Icing Conditions by Radar over an Airport. *FAA In-flight Icing / Ground De-icing International Conference,* Chicago IL, SAA, # 2003-01-2095.

Fabry, F. and I. Zawadzki, 1995: Long-Term Radar Observations of the Melting Layer of Precipitation and Their Interpretation, *Journal of Atmospheric Science*, **52,** 838-851.

Fabry, F., W. Szyrmer, 1999: Modeling of the Melting Layer. Part II: Electromagnetic**.** *Journal of the Atmospheric Sciences*:, **56**, 3593–3600.

Hallett, J., G. Isaac, M. Politovich, D. Marcotte, A. Reehorst, and C. Ryerson, 2002: Alliance Icing Research Study II (AIRS II) science plan. Available at *http://www.airs-icing.org/.*

Lilly, J., 2004: *Detection of in-flight icing conditions through the analysis of hydrometeors with a vertically pointing radar*, Master's thesis, McGill University.

Paull, G., and E. Hagy, 1999: Historical Overview of InFlight Icing Accidents. Contractor report TR-9854/01-1 to the federal Aviation Administration (AUA-460), contract Number: DTRS-57-D00070, 43pp..

Petty, K.R., J.T. Skeen, Jr., G.D. Salottolo, and C.D.J. Floyd. 2003: The Role of the NBTS in Aviation Icing Accident Investigations. *FAA In-flight Icing / Ground De-icing International Conference*, Chicago IL, SAA, # 2003-01-2086.

Stewart, R.E., J.D. Marwitz, J.C. Pace, and R.E. Carbone, 1984: Characteristics through the Melting Layer of Stratiform Clouds, *Journal of Atmospheric Science*, **41,** 3227-3237.

Vecei,. D., 2002: Detection of Supercooled cloud by Radar: Algorithm Comparisons with Aircraft data, Master's thesis, McGill University, 84pp..

Zawadzki, I., W. Szyrmer, S. Laroche, 2000: Diagnostic of supercooled clouds from single-Doppler observations in regions of radar-detectable snow. *Journal of Applied Meteorology,* **39**, 1041-1058.